Published for SISSA by Springer

Received: August 19, 2019
Revised: October 22, 2019
Accepted: November 26, 2019
Published: December 10, 2019

Angular analysis of $\Lambda_b \to \Lambda_c(\to \Lambda\pi)\ell\bar{\nu}$

P. Böer,[a] **A. Kokulu,**[a] **J.-N. Toelstede**[a,b] **and D. van Dyk**[a]

[a] *Physik Department, Technische Universität München, James-Franck-Straße 1, D-85748 Garching, Germany*
[b] *Max-Planck-Institute for Physics, Föhringer Ring 6, D-80805 Munich, Germany*

E-mail: philipp.boeer@tum.de, ahmetkokulu@gmail.com, jan.toelstede@tum.de, danny.van.dyk@gmail.com

Abstract: We revisit the decay $\Lambda_b^0 \to \Lambda_c^+ \ell^- \bar{\nu}$ ($\ell = e, \mu, \tau$) with a subsequent two-body decay $\Lambda_c^+ \to \Lambda^0 \pi^+$ in the Standard Model and in generic New Physics models. The decay's joint four-differential angular distribution can be expressed in terms of ten angular observables, assuming negligible polarization of the initial Λ_b state. We present compact analytical results for all angular observables, which enables us to discuss their possible New Physics reach. We find that the decay at hand probes more and complementary independent combinations of Wilson coefficients compared to its mesonic counter parts $\bar{B} \to D^{(*)}\ell^-\bar{\nu}$. Our result for the angular distribution disagrees with some of the results on scalar-vector interference terms in the literature. We provide numerical estimates for all angular observables based on lattice QCD results for the $\Lambda_b \to \Lambda_c$ form factors and account for a recent measurement of the parity-violating parameter in $\Lambda_c^+ \to \Lambda^0\pi^+$ decays by BESIII. A numerical implementation of our results is made publicly available as part of the EOS software.

Keywords: Beyond Standard Model, Heavy Quark Physics

ArXiv ePrint: 1907.12554

https://doi.org/10.1007/JHEP12(2019)082

JHEP12(2019)082

Contents

JHEP12(2019)082

1 Introduction

Anomalous measurements [1–9] in observables that probe Lepton Flavour Universality (LFU) in $\bar{B} \to D^{(*)}\tau^-\bar{\nu}$ decays motivate careful reappraisal of the theoretical inputs [10–22] entering the present Standard Model (SM) predictions of these decays. At the same time, they also motivate further phenomenological analyses to uncover new observables that complement the LFU probes [23–27], either in terms of independent systematic uncertainties, or in terms of independent constraints on the origin of LFU effects. This work aims to achieve the latter objective by studying the four-differential decay rate of the cascade process[1] $\Lambda_b^0 \to \Lambda_c^+(\to \Lambda^0\pi^+)\ell^-\bar{\nu}$, with any charged lepton species $\ell = e, \mu, \tau$. To achieve this goal, we work within the most general effective theory of local $b \to c\ell\bar{\nu}$ operators with left-handed neutrinos and up to mass dimension six, which includes scalar and tensor interactions besides the SM contributions. Our work extends earlier studies of the three-body decay $\Lambda_b^0 \to \Lambda_c^+\ell^-\bar{\nu}$ [31], and of the four-body decay $\Lambda_b^0 \to \Lambda_c^+(\to \Lambda^0\pi^+)\ell^-\bar{\nu}$ [32, 33]. Our analysis follows closely previous works on the flavour-changing neutral-current decay $\Lambda_b^0 \to \Lambda^0(\to p\pi^-)\ell^+\ell^-$ [34–36], which has a qualitatively similar angular distribution. The LHCb experiment can only reconstruct the decay mode at hand by reconstructing $\Lambda^0 \to p\pi^-$ decays, which correspond to $\simeq 64\%$ of the Λ^0 branching fraction [37]. To assess LHCb's ability to measure the four-differential rate, we estimate the expected signal yield of cascade decays by relating it to the signal yield of $\Lambda_b^0 \to \Lambda_c^+(\to pK^-\pi^+)\mu^-\bar{\nu}$ [29]. Generally, reconstruction of a three-particle final state is less efficient than of a two-particle final

[1] Note that previous analyses of $\Lambda_b^0 \to \Lambda_c^+\ell^-\bar{\nu}$ decays at LHCb used the three-body decay $\Lambda_c^+ \to pK^-\pi^+$ for the reconstruction of the Λ_c^+ [28–30].

state. For the purpose of our estimate, we will treat the reconstruction efficiencies for both Λ_c^+ decay modes as equal. (Any more sophisticated estimate would require LHCb-internal information that is unavailable to us.) Using the world average for the Λ_c^+ branching fractions, we obtain a rough estimate of the signal yield as:

$$\begin{aligned} N(\Lambda_b^0 \to \Lambda_c^+(\to \Lambda^0\pi^+)\mu^-\bar{\nu}) &\simeq N(\Lambda_b^0 \to \Lambda_c^+(\to pK^-\pi^+)\mu^-\bar{\nu}) \times \frac{\mathcal{B}(\Lambda_c^+ \to \Lambda^0\pi^+)}{\mathcal{B}(\Lambda_c^+ \to pK^-\pi^+)} \\ &\simeq 0.5 \cdot 10^6 \,. \end{aligned} \tag{1.1}$$

This corresponds to ten times the signal yield of $\Lambda_b \to \Lambda_c^*(2625)\mu^-\bar{\nu}$ decays, for which a sensitivity study established that a full angular analysis is possible [26]. Hence, we expect excellent prospects for a precision angular analysis of the cascade decay at LHCb in case of the muon mode.

The remainder of this document is structured as follows. We present and discuss our analytical results for the four-body differential decay rate and the ten angular observables arising from the latter in section 2. In section 3 we provide numerical results for the angular observables based on lattice QCD results for the full set of $\Lambda_b \to \Lambda_c$ form factors [31, 38] at mass dimension six, and based on our own average of the parity violating parameter α in the secondary decay $\Lambda_c^+ \to \Lambda^0\pi^+$ [39]. We conclude in section 4.

2 Analytical results

We work within an effective field theory for semileptonic flavour-changing $|\Delta B| = |\Delta C| = 1$ transitions. Its effective Hamiltonian can be expressed as

$$\mathcal{H}^{\text{eff}} = \frac{4\tilde{G}_F}{\sqrt{2}}\tilde{V}_{cb}\left[\sum_i \mathcal{C}_i\mathcal{O}_i\right] , \tag{2.1}$$

where a basis of operators up to mass dimension six and with only left-handed neutrinos can be chosen as

$$\begin{aligned} \mathcal{O}_{V,L(R)} &\equiv \left[\bar{c}\gamma^\mu P_{L(R)}b\right]\left[\bar{\ell}\gamma_\mu P_L\nu_\ell\right] , \quad \mathcal{O}_{S,L(R)} \equiv \left[\bar{c}P_{L(R)}b\right]\left[\bar{\ell}P_L\nu_\ell\right] , \\ \mathcal{O}_T &\equiv \left[\bar{c}\sigma^{\mu\nu}b\right]\left[\bar{\ell}\sigma_{\mu\nu}P_L\nu_\ell\right] . \end{aligned} \tag{2.2}$$

This approach is the standard way to account model-independently for the effects of New Physics (NP). The SM corresponds to the parameter point $\mathcal{C}_{V_L} = 1$ and $\mathcal{C}_j = 0$ for all remaining operators. In the SM the product of parameters $\tilde{G}_F\tilde{V}_{cb}$ coincides with the product of the Fermi constant as extracted from leptonic μ decays and the CKM matrix element V_{cb}. Beyond the SM, they merely provide a common normalization for the effective operators. Throughout this work the value of $\tilde{G}_F \times \tilde{V}_{cb}$ is not relevant for numerical estimates, since it cancels in the angular distribution. However, we emphasize that value becomes relevant when interpreting external inputs for the Wilson coefficients, such as benchmark NP points taken from other works. We note in passing that any interpretation of NP constraints in terms of the Wilson coefficients $\mathcal{C}_i$ within the SM Effective Field Theory requires a careful interpretation of $\tilde{V}_{cb}$ [40].

JHEP12(2019)082

2.1 Angular distribution

Following ref. [34], we express the kinematics of the four-body decay distribution in terms of q^2, the square of the dilepton mass; $\cos\theta_\ell$, the helicity angle of the charged lepton in the dilepton center-of-mass frame; $\cos\theta_{\Lambda_c}$, the helicity angle of the Λ^0 baryon in the $\Lambda^0\pi^+$ center-of-mass frame; and ϕ, the azimuthal angle between the two decay planes. For more details, we refer to appendix A. The fourfold differential distribution takes the form

$$K(q^2, \cos\theta_\ell, \cos\theta_{\Lambda_c}, \phi) \equiv \frac{8\pi}{3} \frac{1}{\mathrm{d}\Gamma/\mathrm{d}q^2} \frac{\mathrm{d}^4\Gamma}{\mathrm{d}q^2\, \mathrm{d}\cos\theta_\ell\, \mathrm{d}\cos\theta_{\Lambda_c}\, \mathrm{d}\phi}\,. \tag{2.3}$$

The physical ranges of the kinematical variables are $m_\ell^2 \le q^2 \le (m_{\Lambda_b} - m_{\Lambda_c})^2$, $\cos\theta_{\ell,\Lambda_c} \in [-1, 1]$ and $\phi \in [0, 2\pi]$. The distribution can be decomposed in terms of a set of trigonometric functions

$$\begin{aligned} K(q^2, \cos\theta_\ell, \cos\theta_{\Lambda_c}, \phi) = {} & \big(K_{1ss}\sin^2\theta_\ell + K_{1cc}\cos^2\theta_\ell + K_{1c}\cos\theta_\ell\big) \\ & + \big(K_{2ss}\sin^2\theta_\ell + K_{2cc}\cos^2\theta_\ell + K_{2c}\cos\theta_\ell\big)\cos\theta_{\Lambda_c} \\ & + \big(K_{3sc}\sin\theta_\ell\cos\theta_\ell + K_{3s}\sin\theta_\ell\big)\sin\theta_{\Lambda_c}\sin\phi \\ & + \big(K_{4sc}\sin\theta_\ell\cos\theta_\ell + K_{4s}\sin\theta_\ell\big)\sin\theta_{\Lambda_c}\cos\phi\,, \end{aligned} \tag{2.4}$$

giving rise to ten angular observables $K_i \equiv K_i(q^2)$. Our choice of the normalization in eq. (2.3) imposes an exact relation between two of the angular observables of the first row, $2K_{1ss} + K_{1cc} = 1$. The structure of eq. (2.4) is imposed by angular momentum conservation [34]. It is generally compatible with the findings of refs. [32, 33], that is, we find the same number of independent angular terms based on the results for the angular distribution of refs. [32, 33] as in eq. (2.4).

In the presence of all five effective operators of eq. (2.2), we can express each angular observable as a sesquilinear form of ten amplitudes

$$\{A_{\lambda_m}, A^T_{\lambda_m}\} = \{A_{\perp_t}, A_{\perp_0}, A_{\perp_1}, A_{\parallel_t}, A_{\parallel_0}, A_{\parallel_1}, A^T_{\perp_0}, A^T_{\perp_1}, A^T_{\parallel_0}, A^T_{\parallel_1}\}\,.$$

Here $\lambda = \perp, \parallel$ denotes the transversity state; $m = t$ denotes timelike dilepton state; $m = 0, 1$ denotes the magnitude of the z-component of the dilepton angular momentum in a vector dilepton state; and the T superscript indicates that an amplitude arises only in the presence of tensor operators. For the first row of eq. (2.4) we find:

$$\begin{aligned} \frac{\mathrm{d}\Gamma}{\mathrm{d}q^2} K_{1ss} = {} & \frac{1}{4}\bigg[\left(1 + \frac{m_\ell^2}{q^2}\right)|A_{\perp_1}|^2 + 2|A_{\perp_0}|^2 + 2\frac{m_\ell^2}{q^2}|A_{\perp_t}|^2 + (\perp \leftrightarrow \parallel)\bigg] \\ & - 2\frac{m_\ell}{\sqrt{q^2}}\,\mathrm{Re}\Big\{A^T_{\perp_0}A^*_{\perp_0} + A^T_{\perp_1}A^*_{\perp_1} + (\perp \leftrightarrow \parallel)\Big\} \\ & + \bigg[\left(1 + \frac{m_\ell^2}{q^2}\right)|A^T_{\perp_1}|^2 + 2\frac{m_\ell^2}{q^2}|A^T_{\perp_0}|^2 + (\perp \leftrightarrow \parallel)\bigg]\,, \end{aligned} \tag{2.5}$$

$$\begin{aligned} \frac{\mathrm{d}\Gamma}{\mathrm{d}q^2} K_{1cc} = {} & \frac{1}{2}\bigg[|A_{\perp_1}|^2 + \frac{m_\ell^2}{q^2}\big(|A_{\perp_0}|^2 + |A_{\perp_t}|^2\big) + (\perp \leftrightarrow \parallel)\bigg] \\ & - 2\frac{m_\ell}{\sqrt{q^2}}\,\mathrm{Re}\Big\{A^T_{\perp_0}A^*_{\perp_0} + A^T_{\perp_1}A^*_{\perp_1} + (\perp \leftrightarrow \parallel)\Big\} \\ & + 2\bigg[|A^T_{\perp_0}|^2 + \frac{m_\ell^2}{q^2}|A^T_{\perp_1}|^2 + (\perp \leftrightarrow \parallel)\bigg]\,, \end{aligned} \tag{2.6}$$

JHEP12(2019)082

$$\frac{\mathrm{d}\Gamma}{\mathrm{d}q^2}K_{1c} = \mathrm{Re}\left\{A_{\perp_1}A^*_{\parallel_1} + \frac{m_\ell^2}{q^2}\left(A_{\perp_0}A^*_{\perp_t} + A_{\parallel_0}A^*_{\parallel_t}\right)\right\} \tag{2.7}$$
$$- 2\frac{m_\ell}{\sqrt{q^2}}\,\mathrm{Re}\left\{A^T_{\perp_0}A^*_{\perp_t} + A^T_{\perp_1}A^*_{\parallel_1} + (\perp \leftrightarrow \parallel)\right\}$$
$$+ 4\frac{m_\ell^2}{q^2}\,\mathrm{Re}\left\{A^T_{\perp_1}A^{T*}_{\parallel_1}\right\}.$$

For the second row of eq. (2.4) we find:

$$\frac{\mathrm{d}\Gamma}{\mathrm{d}q^2}K_{2ss} = \frac{\alpha}{2}\,\mathrm{Re}\left\{\left(1+\frac{m_\ell^2}{q^2}\right)A_{\perp_1}A^*_{\parallel_1} + 2A_{\perp_0}A^*_{\parallel_0} + 2\frac{m_\ell^2}{q^2}A_{\perp_t}A^*_{\parallel_t}\right\} \tag{2.8}$$
$$- 2\,\alpha\frac{m_\ell}{\sqrt{q^2}}\,\mathrm{Re}\left\{A^T_{\perp_0}A^*_{\parallel_0} + A^T_{\perp_1}A^*_{\parallel_1} + (\perp \leftrightarrow \parallel)\right\}$$
$$+ 2\,\alpha\,\mathrm{Re}\left\{\left(1+\frac{m_\ell^2}{q^2}\right)A^T_{\perp_1}A^{T*}_{\parallel_1} + 2\frac{m_\ell^2}{q^2}A^T_{\perp_0}A^{T*}_{\parallel_0}\right\},$$

$$\frac{\mathrm{d}\Gamma}{\mathrm{d}q^2}K_{2cc} = \alpha\,\mathrm{Re}\left\{A_{\perp_1}A^*_{\parallel_1} + \frac{m_\ell^2}{q^2}\left(A_{\perp_0}A^*_{\parallel_0} + A_{\perp_t}A^*_{\parallel_t}\right)\right\} \tag{2.9}$$
$$- 2\,\alpha\frac{m_\ell}{\sqrt{q^2}}\,\mathrm{Re}\left\{A^T_{\perp_0}A^*_{\parallel_0} + A^T_{\perp_1}A^*_{\parallel_1} + (\perp \leftrightarrow \parallel)\right\}$$
$$+ 4\,\alpha\,\mathrm{Re}\left\{A^T_{\perp_0}A^{T*}_{\parallel_0} + \frac{m_\ell^2}{q^2}A^T_{\perp_1}A^{T*}_{\parallel_1}\right\},$$

$$\frac{\mathrm{d}\Gamma}{\mathrm{d}q^2}K_{2c} = \frac{\alpha}{2}\left[|A_{\perp_1}|^2 + 2\frac{m_\ell^2}{q^2}\,\mathrm{Re}\left\{A_{\perp_0}A^*_{\parallel_t}\right\} + (\perp \leftrightarrow \parallel)\right] \tag{2.10}$$
$$- 2\,\alpha\frac{m_\ell}{\sqrt{q^2}}\,\mathrm{Re}\left\{A^T_{\perp_0}A^*_{\parallel_t} + A^T_{\perp_1}A^*_{\perp_1} + (\perp \leftrightarrow \parallel)\right\}$$
$$+ 2\,\alpha\frac{m_\ell^2}{q^2}\left[|A^T_{\perp_1}|^2 + (\perp \leftrightarrow \parallel)\right].$$

For the third row of eq. (2.4) we find:

$$\frac{\mathrm{d}\Gamma}{\mathrm{d}q^2}K_{3sc} = -\frac{\alpha}{\sqrt{2}}\left(1-\frac{m_\ell^2}{q^2}\right)\mathrm{Im}\left\{A_{\perp_0}A^*_{\perp_1} - (\perp \leftrightarrow \parallel)\right\} \tag{2.11}$$
$$+ 2\sqrt{2}\,\alpha\left(1-\frac{m_\ell^2}{q^2}\right)\mathrm{Im}\left\{A^T_{\perp_0}A^{T*}_{\perp_1} - (\perp \leftrightarrow \parallel)\right\},$$

$$\frac{\mathrm{d}\Gamma}{\mathrm{d}q^2}K_{3s} = -\frac{\alpha}{\sqrt{2}}\,\mathrm{Im}\left\{A_{\perp_0}A^*_{\parallel_1} + \frac{m_\ell^2}{q^2}A_{\perp_1}A^*_{\perp_t} - (\perp \leftrightarrow \parallel)\right\} \tag{2.12}$$
$$+ \sqrt{2}\,\alpha\frac{m_\ell}{\sqrt{q^2}}\,\mathrm{Im}\left\{A^T_{\perp_0}A^*_{\parallel_1} + A^T_{\perp_1}A^*_{\parallel_0} + A^T_{\perp_1}A^*_{\perp_t} - (\perp \leftrightarrow \parallel)\right\}$$
$$- 2\sqrt{2}\,\alpha\frac{m_\ell^2}{q^2}\,\mathrm{Im}\left\{A^T_{\perp_0}A^{T*}_{\parallel_1} - (\perp \leftrightarrow \parallel)\right\}.$$

For the fourth row of eq. (2.4) we find:

$$\frac{\mathrm{d}\Gamma}{\mathrm{d}q^2}K_{4sc} = -\frac{\alpha}{\sqrt{2}}\left(1-\frac{m_\ell^2}{q^2}\right)\mathrm{Re}\left\{A_{\perp_0}A^*_{\parallel_1} - (\perp \leftrightarrow \parallel)\right\} \tag{2.13}$$
$$+ 2\sqrt{2}\,\alpha\left(1-\frac{m_\ell^2}{q^2}\right)\mathrm{Re}\left\{A^T_{\perp_0}A^{T*}_{\parallel_1} - (\perp \leftrightarrow \parallel)\right\},$$

JHEP12(2019)082

$$\frac{\mathrm{d}\Gamma}{\mathrm{d}q^2} K_{4s} = -\frac{\alpha}{\sqrt{2}} \mathrm{Re}\left\{ A_{\perp_0} A^*_{\perp_1} + \frac{m_\ell^2}{q^2} A_{\perp_1} A^*_{\|_t} - (\perp \leftrightarrow \|) \right\} \tag{2.14}$$
$$+ \sqrt{2}\,\alpha \frac{m_\ell}{\sqrt{q^2}} \mathrm{Re}\left\{ A^T_{\perp_0} A^*_{\perp_1} + A^T_{\perp_1} A^*_{\perp_0} + A^T_{\perp_1} A^*_{\|_t} - (\perp \leftrightarrow \|) \right\}$$
$$- 2\sqrt{2}\,\alpha \frac{m_\ell^2}{q^2} \mathrm{Re}\left\{ A^T_{\perp_0} A^{T*}_{\perp_1} - (\perp \leftrightarrow \|) \right\} .$$

Note that the two observables K_{3sc} and K_{3s} vanish when analyzing the combined Λ_b^0 and $\bar{\Lambda}_b^0$ angular distribution; their extraction therefore requires separation of the two modes. Comparing our results to the literature, our findings are summarized as follows:

- We find complete agreement with the results of ref. [31], which discusses the *non-cascade* decay in the presence of all dimension-six operators.

- Our findings disagree with the results of ref. [32], which discusses the cascasde decay for all dimension-six operators *except* for the tensor operator. We find interference terms of the type $V \times S$ and $A \times P$ in our angular observables K_{3s} and K_{4s} that are absent from the corresponding term C_4^{int} of ref. [32, arXiv v4]. We believe our results to be correct, since they pass a crucial cross check: the interference between vector and scalar operators can be completely described by a shift of the timelike transversity amplitudes $A_{\perp_t}$ and $A_{\|_t}$. This shift is consistent with a Ward-like identity for the $\Lambda_b \to \Lambda_c$ matrix elements:

$$\langle \Lambda_c | \, \bar{c}(\gamma_5)\, b \, | \Lambda_b \rangle = \frac{q^\mu}{m_b \mp m_c} \langle \Lambda_c | \, \bar{c}(\gamma_5) \gamma_\mu b \, | \Lambda_b \rangle \ . \tag{2.15}$$

  The term C_4^{int} in eq. (19) of ref. [32] cannot be expressed through this shift. Additionally, we find a lack of an overall multiplicative factor $\mathcal{B}(\Lambda_c^+ \to \Lambda^0 \pi^+)$ from the secondary decay. Furthermore, we find agreement only by redefining the angles $\theta_\ell \to \pi - \theta_\ell$, $\theta_{\Lambda_c} \to \theta_s$ and $\phi \to -\chi$.

- Comparing our results to the SM results for the fourfold distribution in ref. [33], we find complete agreement when redefining the angles as $\theta_\ell \to \pi - \theta_\ell$, $\theta_{\Lambda_c} \to \theta_s$ and $\phi \to -\chi$. We note the absence of any terms corresponding to the angular observables K_{3sc} and K_{3s}, which vanish in the SM.

Our results therefore provide for the first time the full angular distribution of the cascade decay in the presence of all dimension-six operators with left-handed neutrinos.

In the definition of seven out of the ten angular observables in eq. (2.4), we explicitly factor out the quantity $\alpha \equiv \alpha(\Lambda_c^+ \to \Lambda^0 \pi^+)$, which is an angular asymmetry parameter arising in $\Lambda_c^+ \to \Lambda^0 \pi^+$ decays. It emerges as the hadronic matrix element of the parity-violating weak decay of the Λ_c^+. The present world average of this parameter by the Particle Data Group (PDG) [37] reads:

$$\alpha^{\mathrm{PDG}} = -0.91 \pm 0.15 \, . \tag{2.16}$$

JHEP12(2019)082

It includes measurements by the CLEO [41] and ARGUS [42] experiments, in addition to the statistically dominating measurements by the CLEO-2 [43] e^+e^- collider experiment,

$$\alpha^{\text{CLEO-2}} = -0.94 \pm 0.21(\text{stat.}) \pm 0.12(\text{syst.})\,, \tag{2.17}$$

and by the FOCUS (Fermilab E-831) [44] fixed target experiment,

$$\alpha^{\text{FOCUS}} = -0.78 \pm 0.16(\text{stat.}) \pm 0.13(\text{syst.})\,. \tag{2.18}$$

With the recent measurement of α by the BESIII collaboration in e^+e^- collisions,

$$\alpha^{\text{BESIII}} = -0.80 \pm 0.11(\text{stat.}) \pm 0.02(\text{syst.})\,, \tag{2.19}$$

we compute our own average including also the CLEO-2 and FOCUS results. We obtain:

$$\alpha = -0.82 \pm 0.09 \tag{2.20}$$

In the following we will use this average in lieu of an updated world average by the PDG.

2.2 Transversity amplitudes

The transversity amplitudes arising in the angular observables K_i are further decomposed into $\Lambda_b \to \Lambda_c$ helicity form factors as defined in ref. [45], Wilson coefficients, and kinematical factors. Equations of motion for the b and c-quark fields relate the hadronic matrix elements of scalar (pseudo-scalar) currents to timelike vector (axial-vector) form factors. In the absence of the tensor operator we find six independent transversity amplitudes:

$$A_{\perp_1} = -2\mathcal{N}\sqrt{s_-}\, f_\perp^V(q^2)\, \mathcal{C}_{V,+} \equiv F_{\perp_1}\, \mathcal{C}_{V,+}\,, \tag{2.21}$$

$$A_{\parallel_1} = +2\mathcal{N}\sqrt{s_+}\, f_\perp^A(q^2)\, \mathcal{C}_{V,-} \equiv F_{\parallel_1}\, \mathcal{C}_{V,-}\,, \tag{2.22}$$

$$A_{\perp_0} = +\sqrt{2}\mathcal{N}\sqrt{s_-}\frac{m_{\Lambda_b}+m_{\Lambda_c}}{\sqrt{q^2}}\, f_0^V(q^2)\, \mathcal{C}_{V,+} \equiv F_{\perp_0}\, \mathcal{C}_{V,+}\,, \tag{2.23}$$

$$A_{\parallel_0} = -\sqrt{2}\mathcal{N}\sqrt{s_+}\frac{m_{\Lambda_b}-m_{\Lambda_c}}{\sqrt{q^2}}\, f_0^A(q^2)\, \mathcal{C}_{V,-} \equiv F_{\parallel_0}\, \mathcal{C}_{V,-}\,, \tag{2.24}$$

$$\begin{aligned} A_{\perp_t} &= +\sqrt{2}\mathcal{N}\sqrt{s_+}\frac{m_{\Lambda_b}-m_{\Lambda_c}}{m_\ell}\, f_t^V(q^2) \left[\frac{m_\ell}{\sqrt{q^2}}\,\mathcal{C}_{V,+} + \frac{\sqrt{q^2}}{m_b-m_c}\,\mathcal{C}_{S,+}\right] \\ &\equiv F_{\perp_t}\,\mathcal{C}_{V,+} + \frac{\sqrt{q^2}}{m_\ell} F_\perp^S\,\mathcal{C}_{S,+}\,, \end{aligned} \tag{2.25}$$

$$\begin{aligned} A_{\parallel_t} &= -\sqrt{2}\mathcal{N}\sqrt{s_-}\frac{m_{\Lambda_b}+m_{\Lambda_c}}{m_\ell}\, f_t^A(q^2) \left[\frac{m_\ell}{\sqrt{q^2}}\,\mathcal{C}_{V,-} - \frac{\sqrt{q^2}}{m_b+m_c}\,\mathcal{C}_{S,-}\right] \\ &\equiv F_{\parallel_t}\,\mathcal{C}_{V,-} + \frac{\sqrt{q^2}}{m_\ell} F_\parallel^S\,\mathcal{C}_{S,-}\,, \end{aligned} \tag{2.26}$$

with

$$s_\pm \equiv \left(m_{\Lambda_b} \pm m_{\Lambda_c}\right)^2 - q^2\,. \tag{2.27}$$

JHEP12(2019)082

We note that the timelike leptonic polarization state requires a non-vanishing lepton mass. Hence, the transversity amplitudes $A_{\perp_t}$ and $A_{\parallel_t}$ always enter observables with a factor m_ℓ such that all physical observables are well-defined in the limit $m_\ell \to 0$. In the above we introduce a phenomenologically useful basis of effective form factors F_{λ_m} and F_λ^S, and abbreviate common linear combinations of the Wilson coefficients:

$$\mathcal{C}_{V,\pm} \equiv \mathcal{C}_{V,L} \pm \mathcal{C}_{V,R}\,, \qquad\qquad \mathcal{C}_{S,\pm} \equiv \mathcal{C}_{S,L} \pm \mathcal{C}_{S,R}\,. \tag{2.28}$$

We also introduce an overall normalization factor

$$\mathcal{N} \equiv \tilde{G}_F\, \tilde{V}_{cb} \left(1 - \frac{m_\ell^2}{q^2}\right) \sqrt{\frac{q^2 \sqrt{\lambda(m_{\Lambda_b}^2, m_{\Lambda_c}^2, q^2)}}{3 \times 2^7 \pi^3 m_{\Lambda_b}^3} \times \mathcal{B}(\Lambda_c^+ \to \Lambda^0 \pi^+)}\,, \tag{2.29}$$

with the Källén function $\lambda(a,b,c) = a^2 + b^2 + c^2 - 2ab - 2ac - 2bc$.

In the presence of the tensor operator we find four additional transversity amplitudes and hence four additional effective form factors $F_{\lambda_m}^T$:

$$A_{\parallel_0}^T = -2\sqrt{2}\mathcal{N}\sqrt{s_+}\,\mathcal{C}_T f_0^{T5}(q^2) \equiv F_{\parallel_0}^T\,\mathcal{C}_T\,, \tag{2.30}$$

$$A_{\perp_0}^T = -2\sqrt{2}\mathcal{N}\sqrt{s_-}\,\mathcal{C}_T f_0^{T}(q^2) \equiv F_{\perp_0}^T\,\mathcal{C}_T\,, \tag{2.31}$$

$$A_{\parallel_1}^T = +4\mathcal{N}\frac{m_{\Lambda_b} - m_{\Lambda_c}}{\sqrt{q^2}}\sqrt{s_+}\,\mathcal{C}_T f_\perp^{T5}(q^2) \equiv F_{\parallel_1}^T\,\mathcal{C}_T\,, \tag{2.32}$$

$$A_{\perp_1}^T = +4\mathcal{N}\frac{m_{\Lambda_b} + m_{\Lambda_c}}{\sqrt{q^2}}\sqrt{s_-}\,\mathcal{C}_T f_\perp^{T}(q^2) \equiv F_{\perp_1}^T\,\mathcal{C}_T\,. \tag{2.33}$$

2.3 Phenomenology

To understand the NP reach of any of the angular observables or their combinations, it is instrumental to understand the sesquilinear combinations of Wilson coefficients entering the observables. To facilitate this understanding we define five real-valued and ten complex-valued quantities σ:

$$\begin{aligned}
\sigma_{V,1}^{\pm} &= \frac{1}{2}|\mathcal{C}_{V,\pm}|^2\,, & \sigma_{V,2} &= -\mathcal{C}_{V,-}\mathcal{C}_{V,+}^*\,,\\
\sigma_{S,1}^{\pm} &= \frac{1}{2}|\mathcal{C}_{S,\pm}|^2\,, & \sigma_{S,2} &= -\mathcal{C}_{S,-}\mathcal{C}_{S,+}^*\,,\\
\sigma_{VS,1}^{\pm} &= \frac{1}{2}\mathcal{C}_{V,\pm}\mathcal{C}_{S,\pm}^*\,, & \sigma_{VS,2} &= -\mathcal{C}_{V,-}\mathcal{C}_{S,+}^*\,,\\
& & \sigma_{SV,2} &= -\mathcal{C}_{S,-}\mathcal{C}_{V,+}^*\,,\\
\sigma_{T,1} &= \frac{1}{2}|\mathcal{C}_T|^2\,, & & \\
\sigma_{VT,1}^{\pm} &= \frac{1}{2}\mathcal{C}_{V,\pm}\mathcal{C}_T^*\,, & & \\
\sigma_{ST,1}^{\pm} &= \frac{1}{2}\mathcal{C}_{S,\pm}\mathcal{C}_T^*\,. & &
\end{aligned} \tag{2.34}$$

JHEP12(2019)082

This constitutes the complete set of sesquilinear combinations of the Wilson coefficients, and corresponds to 25 real-valued degrees of freedom. In terms of these combinations and effective form factors, we find in the limit $m_\ell \to 0$

$$\frac{\mathrm{d}\Gamma}{\mathrm{d}q^2}K_{1ss} = \frac{1}{2}\sigma^+_{V,1}\Big(2\,|F_{\perp_0}|^2 + |F_{\perp_1}|^2\Big) + \frac{1}{2}\sigma^-_{V,1}\Big(2\,|F_{\parallel_0}|^2 + |F_{\parallel_1}|^2\Big) \tag{2.35}$$
$$+ 4\Big(\sigma^+_{S,1}|F^S_\perp|^2 + \sigma^-_{S,1}|F^S_\parallel|^2\Big) + 2\,\sigma_{T,1}\Big(|F^T_{\perp_1}|^2 + |F^T_{\parallel_1}|^2\Big)\,,$$

$$\frac{\mathrm{d}\Gamma}{\mathrm{d}q^2}K_{1cc} = \sigma^+_{V,1}|F_{\perp_1}|^2 + \sigma^-_{V,1}|F_{\parallel_1}|^2 + \sigma^+_{S,1}|F^S_\perp|^2 + \sigma^-_{S,1}|F^S_\parallel|^2 \tag{2.36}$$
$$+ 4\,\sigma_{T,1}\Big(|F^T_{\perp_0}|^2 + |F^T_{\parallel_0}|^2\Big)\,,$$

$$\frac{\mathrm{d}\Gamma}{\mathrm{d}q^2}K_{1c} = -\,\mathrm{Re}\left\{\sigma_{V,2}F_{\parallel_1}F^*_{\perp_1} + 4\,\sigma^+_{ST,1}F^S_\perp F^{T*}_{\perp_0} + 4\,\sigma^-_{ST,1}F^S_\parallel F^{T*}_{\parallel_0}\right\}, \tag{2.37}$$

$$\frac{\mathrm{d}\Gamma}{\mathrm{d}q^2}K_{2ss} = -\frac{\alpha}{2}\,\mathrm{Re}\left\{\sigma_{V,2}\Big(F_{\parallel_1}F^*_{\perp_1} + 2\,F_{\parallel_0}F^*_{\perp_0}\Big) + 2\,\sigma_{S,2}F^S_\parallel F^{S*}_\perp - 8\,\sigma_{T,1}F^T_{\parallel_1}F^{T*}_{\perp_1}\right\} \tag{2.38}$$

$$\frac{\mathrm{d}\Gamma}{\mathrm{d}q^2}K_{2cc} = -\alpha\,\mathrm{Re}\left\{\sigma_{V,2}F_{\parallel_1}F^*_{\perp_1} + \sigma_{S,2}F^S_\parallel F^{S*}_\perp - 8\,\alpha\,\sigma_{T,1}F^T_{\parallel_0}F^{T*}_{\perp_0}\right\}, \tag{2.39}$$

$$\frac{\mathrm{d}\Gamma}{\mathrm{d}q^2}K_{2c} = \alpha\Big(\sigma^+_{V,1}|F_{\perp_1}|^2 + \sigma^-_{V,1}|F_{\parallel_1}|^2\Big) - 4\,\alpha\,\mathrm{Re}\left\{\sigma^+_{ST,1}F^S_\perp F^{T*}_{\parallel_0} + \sigma^-_{ST,1}F^S_\parallel F^{T*}_{\perp_0}\right\}, \tag{2.40}$$

$$\frac{\mathrm{d}\Gamma}{\mathrm{d}q^2}K_{3sc} = -\sqrt{2}\,\alpha\,\mathrm{Im}\left\{\sigma^+_{V,1}F_{\perp_0}F^*_{\perp_1} - \sigma^-_{V,1}F_{\parallel_0}F^*_{\parallel_1} - 4\,\sigma_{T,1}\Big(F^T_{\perp_0}F^{T*}_{\perp_1} - F^T_{\parallel_0}F^{T*}_{\parallel_1}\Big)\right\}, \tag{2.41}$$

$$\frac{\mathrm{d}\Gamma}{\mathrm{d}q^2}K_{3s} = -\frac{\alpha}{\sqrt{2}}\,\mathrm{Im}\left\{\sigma_{V,2}\Big(F_{\parallel_1}F^*_{\perp_0} + F_{\parallel_0}F^*_{\perp_1}\Big) + 4\,\sigma^+_{ST,1}F^S_\perp F^{T*}_{\perp_1} - 4\,\sigma^-_{ST,1}F^S_\parallel F^{T*}_{\parallel_1}\right\}, \tag{2.42}$$

$$\frac{\mathrm{d}\Gamma}{\mathrm{d}q^2}K_{4sc} = \frac{\alpha}{\sqrt{2}}\,\mathrm{Re}\left\{\sigma_{V,2}\Big(F_{\parallel_1}F^*_{\perp_0} - F_{\parallel_0}F^*_{\perp_1}\Big) + 8\,\sigma_{T,1}\Big(F^T_{\perp_0}F^{T*}_{\parallel_1} - F^T_{\parallel_0}F^{T*}_{\perp_1}\Big)\right\}, \tag{2.43}$$

$$\frac{\mathrm{d}\Gamma}{\mathrm{d}q^2}K_{4s} = -\sqrt{2}\,\alpha\,\mathrm{Re}\left\{\sigma^+_{V,1}F_{\perp_0}F^*_{\perp_{-1}} - \sigma^-_{V,1}F_{\parallel_0}F^*_{\parallel_1}\right\} \tag{2.44}$$
$$- 2\,\sqrt{2}\,\alpha\,\mathrm{Re}\left\{\sigma^+_{ST,1}F^S_\perp F^{T*}_{\parallel_1} - 2\,\sigma^-_{ST,1}F^S_\parallel F^{T*}_{\perp_1}\right\}.$$

The result above illustrates that the cascade decay for $\ell = e, \mu$ is sensitive to 12 out of the 25 real-valued combinations of Wilson coefficients:

$$\Sigma(m_\ell = 0) \equiv \{\sigma^\pm_{V,1}, \sigma^\pm_{S,1}, \sigma_{T,1}, \mathrm{Re}\,\sigma_{V,2}, \mathrm{Im}\,\sigma_{V,2}, \mathrm{Re}\,\sigma_{S,2}, \mathrm{Re}\,\sigma^\pm_{ST,1}, \mathrm{Im}\,\sigma^\pm_{ST,1}\}\,.$$

This sensitivity should be compared to the sensitivity exhibited by $\bar{B} \to D^{(*)}\ell^-\bar{\nu}$ decays. For the pseudoscalar final state meson, the coefficients $\mathcal{C}_{V,-}$ and $\mathcal{C}_{S,-}$ do not enter at all by virtue of vanishing matrix elements. For the vector final state meson, the coefficient $\mathcal{C}_{S,+}$ does not enter for the same reason. Hence, not all elements of $\Sigma(m_\ell = 0)$ are accessible in the B-meson decays, in particular $\sigma_{VS,2}$ and $\sigma_{S,2}$, and therefore the Λ_b cascade decay provides new and complementary constraints on the Wilson coefficients. We refrain from providing lengthy expressions for the massive case $\ell = \tau$, which can be readily obtained from our results in section 2.1. We find that the cascade decay with a massive lepton is

JHEP12(2019)082

sensitive to a larger set of 22 (out of 25) real-valued combinations of Wilson coefficients. The full set of combinations reads:

$$\Sigma \equiv \Sigma(m_\ell = 0) \cup \{\mathrm{Re}\,\sigma^{\pm}_{VS,1}, \mathrm{Im}\,\sigma^{\pm}_{VS,1}, \mathrm{Re}\,\sigma_{VS,2}, \mathrm{Re}\,\sigma_{SV,2}, \mathrm{Re}\,\sigma^{\pm}_{VT,1}, \mathrm{Im}\,\sigma^{\pm}_{VT,1}\}\,.$$

Presently, the only prospect for measurement of the $\Lambda_b^0 \to \Lambda_c^+ \mu^- \bar{\nu}$ decays is the LHCb experiment. Within LHCb, reconstruction of the $\bar{\nu}$ momentum from the remaining initial state and decay kinematics is difficult, but possible [46]. We do not expect a measurement of all ten angular observables before a sufficiently large data set is available. In the mean time, we focus on identifying observables that can be more readily measured than the full angular distribution. The LHCb experiment provides projections of the angular resolution in $\bar{B} \to D^*(\to D\pi)\ell^-\bar{\nu}$ decays [47, section 5.3.1 and figure 5.4], which clearly show that the $D\pi$ helicity angle is the best candidate for reconstruction. Under the assumption that LHCb's performance in the cascade decay reflects the projected performance $\bar{B} \to D^*(\to D\pi)\ell^-\bar{\nu}$, we search for observables that can be determined without reconstruction of either the dilepton helicity angle or the azimuthal angle. Analysis of eq. (2.4) suggests only one angular observable that meets this criterium: the hadronic forward-backward asymmetry,

$$A_{\mathrm{FB}}^{\Lambda_c} \equiv K_{2ss} + \frac{1}{2} K_{2cc}\,. \tag{2.45}$$

Measurement of this observable can be achieved through a counting experiment with respect to the sign of $\cos\theta_{\Lambda_c}$, normalized to the sum of all events. The normalization through the decay rate is helpful in two ways. First, it reduces the inherent theoretical uncertainties by partial cancellation of the (correlated) form factor uncertainties. Second, it reduces systematic experimental uncertainties in the measurement, including the poorly-known Λ_b fragmentation fraction at LHCb. The ability to determine $A_{\mathrm{FB}}^{\Lambda_c}$ regardless of the reconstruction of the lepton helicity angle will also make possible to probe LFU through the ratio:

$$R(A_{\mathrm{FB}}^{\Lambda_c}) \equiv \frac{\left[A_{\mathrm{FB}}^{\Lambda_c}\right]_{\ell=\tau}}{\left[A_{\mathrm{FB}}^{\Lambda_c}\right]_{\ell=\mu}}\,. \tag{2.46}$$

In the above, the $\ell = \tau$ and $\ell = \mu$ subscripts denote that the forward-backward asymmetry is to be extracted from decays into the specific lepton species ℓ. By virtue of taking the LFU ratio as defined in eq. (2.46) the sensitivity to the parity violating parameter α is completely removed.

For further phenomenological applications we provide the full set of angular observables for the full basis of dimension-six operators as part of the `EOS` software [48] as of version 0.2.5.

3 Numerical results

For the numerical illustration we define three NP benchmark points (BMPs). BMP #1 reads:

$$\begin{aligned} \mathcal{C}_{V,L}^{(\tau)} &= 1.15\,, & \mathcal{C}_{V,R}^{(\tau)} &= 0\,, \\ \mathcal{C}_{S,L}^{(\tau)} &= -0.30\,, & \mathcal{C}_{S,R}^{(\tau)} &= +0.30\,, & \mathcal{C}_{T}^{(\tau)} &= 0\,. \end{aligned} \tag{3.1}$$

JHEP12(2019)082

	SM		BMP #1	BMP #2	BMP #3
obs.	$\ell = \mu$	$\ell = \tau$	$\ell = \tau$	$\ell = \tau$	$\ell = \tau$
K_{1cc}	$+0.206 \pm 0.004$	$+0.310 \pm 0.001$	$+0.311 \pm 0.000$	$+0.307 \pm 0.001$	$+0.343 \pm 0.001$
K_{1c}	-0.134 ± 0.004	$+0.016 \pm 0.003$	$+0.037 \pm 0.002$	-0.073 ± 0.002	$+0.080 \pm 0.003$
K_{2ss}	$+0.288 \pm 0.032$	$+0.221 \pm 0.024$	$+0.228 \pm 0.025$	$+0.167 \pm 0.018$	$+0.252 \pm 0.027$
K_{2cc}	$+0.115 \pm 0.013$	$+0.183 \pm 0.020$	$+0.193 \pm 0.021$	$+0.122 \pm 0.013$	$+0.130 \pm 0.013$
K_{2c}	-0.164 ± 0.018	-0.031 ± 0.004	-0.017 ± 0.003	-0.123 ± 0.013	-0.080 ± 0.009
K_{4sc}	$+0.063 \pm 0.008$	$+0.023 \pm 0.003$	$+0.022 \pm 0.002$	$+0.026 \pm 0.003$	$+0.001 \pm 0.000$
K_{4s}	$+0.125 \pm 0.015$	$+0.063 \pm 0.007$	$+0.065 \pm 0.007$	$+0.161 \pm 0.017$	$+0.039 \pm 0.004$

Table 1. Predictions for the angular observables in the SM and in the NP benchmark point. The observable K_{1ss} can be obtained as $(1 - K_{1cc})/2$ and is hence not listed. The observables K_{3sc} and K_{3s} are zero in the SM and in all NP models without new CP-violating phases in the $b \to c\ell\bar{\nu}$ Wilson coefficients.

BMP #2 reads:

$$\begin{aligned} \mathcal{C}_{V,L}^{(\tau)} &= 1.40\,, & \mathcal{C}_{V,R}^{(\tau)} &= 0\,, \\ \mathcal{C}_{S,L}^{(\tau)} &= -1.15\,, & \mathcal{C}_{S,R}^{(\tau)} &= -0.35\,, & \mathcal{C}_{T}^{(\tau)} &= 0.10\,. \end{aligned} \tag{3.2}$$

BMP #3 reads:

$$\begin{aligned} \mathcal{C}_{V,L}^{(\tau)} &= 0.40\,, & \mathcal{C}_{V,R}^{(\tau)} &= 0\,, \\ \mathcal{C}_{S,L}^{(\tau)} &= 0\,, & \mathcal{C}_{S,R}^{(\tau)} &= +0.60\,, & \mathcal{C}_{T}^{(\tau)} &= 0.30\,. \end{aligned} \tag{3.3}$$

All BMPs are inspired by and compatible with the best-fit points labelled "minimum 1" through "minimum 3" in a recent global analysis of the available data on $b \to c\tau\bar{\nu}$ processes [49].

We provide numerical results for the entire set of angular observables integrated over their full q^2 phase space in table 1. Our results include SM predictions for both $\ell = \mu$ and $\ell = \tau$, as well as predictions for the NP benchmark point ($\ell = \tau$ only). We illustrate the q^2 dependence of the hadronic forward-backward asymmetry and the NP reach of its LFU ratio in figure 1. For all predictions we estimate the theoretical uncertainties based on two sets of inputs. First, for the parity violating parameter α — following the discussion in section 2.1 — we use an average that includes the new BESIII measurement in lieu of the world average. Second, for the hadronic form factors we use the lattice QCD results[2] of the full set of form factors based on the tables provided in refs. [31, 50]. We use the `EOS` software [48] for the computation of all numerical values and plots shown in this work.

Benefiting from the correlated results for the $\Lambda_b \to \Lambda_c$ form factors and from cancellations due to the normalization to the decay rate, we find small uncertainties of the order

[2]Note that the numerical results for the tensor form factors obtained from lattice QCD [50] seem to be inconsistent with the numerical results for the remaining form factors obtained using the same method in ref. [31] according to a recent analysis of the heavy-quark expansion to order $1/m_c^2$ [51]. We emphasize that our numerical implementation is agnostic of the parametrization and numerical inputs for the full set of form factors. Our predictions for the benchmark points involving a non-zero $\mathcal{C}_T^{(\tau)}$ should therefore be revisited once this inconsistency is understood.

JHEP12(2019)082

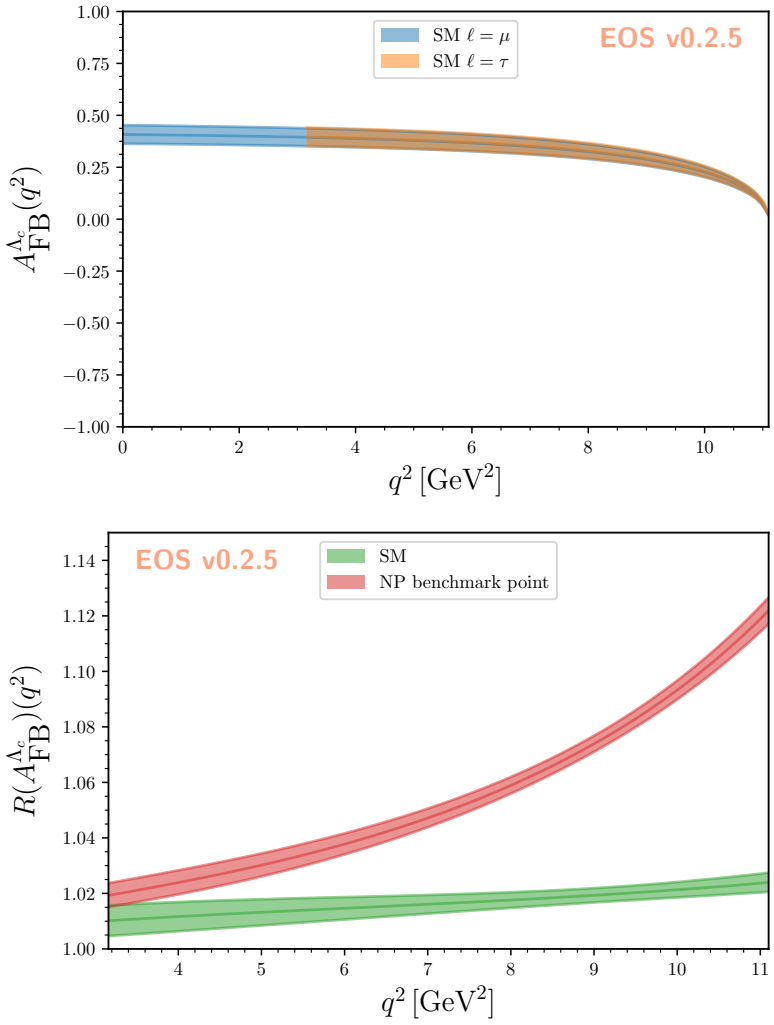

Figure 1. Predictions for (top) the hadronic forward-backward asymmetry in the SM for $\ell = \mu$ and $\ell = \tau$ final states, and (bottom) the LFU ratio $R(A_{\rm FB}^{\Lambda_c})$ in the SM and in the NP benchmark point BMP #1. The bands correspond to the 68% probability envelopes. The theoretical uncertainties are due to the hadronic form factors [50] and the parity violating parameter α (see text). Due to the absence of any threshold effects with respect to the dilepton mass, the two bands for the hadronic forward-backward asymmetry are virtually indistinguishable. The LFU ratio hence exhibits this large sensitivity to the NP benchmark point.

of 11% for $A_{\rm FB}^{\Lambda_c}$ that are dominated by the uncertainty in the parameter α. This becomes much more visible in the LFU ratio where α cancels completely. For that observable the relative uncertainty is reduced to $\sim 1\%$, providing an excellent opportunity for a high-precision probe of New Physics in semileptonic $b \to c$ transitions. We therefore encourage a sensitivity study to determine the experimental precision that the LHCb experiment can achieve for the projected size of the upcoming data sets.

JHEP12(2019)082

4 Summary

We present the first study of the full angular distribution of the cascade decay $\Lambda_b^0 \to \Lambda_c^+(\to \Lambda^0\pi^+)\ell^-\bar{\nu}$ using the complete basis of dimension-six operators, assuming only left-handed neutrinos, in the weak effective field theory for $b \to c\ell\bar{\nu}$ transitions. As a cross check, we reproduce the rate of the non-cascade decay. Our findings disagree with some scalar/vector and pseudoscalar/axialvector interference terms of the four-differential decay rate in the literature. However, our results pass a crucial cross check for amplitudes to timelike polarized dilepton states, which is not fulfilled by the results in the literature.

We express the four-differential rate through a set of ten angular observables, nine of which are independent. The full set of angular observables is shown to be sensitive to more combinations of NP couplings than the decays $\bar{B} \to D\ell\bar{\nu}$ and $\bar{B} \to D^*\ell\bar{\nu}$ taken together. This highlights the usefulness of the cascade decay in constraining potential NP effects in $b \to c\ell\bar{\nu}$ transitions for all lepton species $\ell = e, \mu, \tau$. For convenience, we provide computer code for the numerical evaluation of all angular observables as part of the `EOS` software.

We suggest to measure the hadronic forward-backward asymmetry, which is the only angular observable that can be extracted from the angular distribution without either knowledge of the lepton helicity angle or the azimuthal angle between the decay planes. We expect good prospects for its measurement at the LHCb experiment for all three lepton species. We find that the LFU ratio of the hadronic forward-backward asymmetry features very small hadronic uncertainties in the Standard Model and beyond. It is therefore a prime candidate to cross check the present anomalies in the LFU ratios $R(D)$ and $R(D^*)$.

Acknowledgments

We are grateful to Martin Jung and Marcello Rotondo for helpful comments on the manuscript. This work is supported by the Deutsche Forschungsgemeinschaft (DFG) within the Emmy Noether Programme under grant DY-130/1-1 and the DFG Collaborative Research Center 110 "Symmetries and the Emergence of Structure in QCD".

A Kinematics

We label the momenta in the cascade decay as follows:

$$\Lambda_b^0(p) \to \Lambda_c^+(k)\bar{\nu}_\ell(q_1)\ell^-(q_2)\,, \quad \Lambda_c^+(k) \to \Lambda^0(k_1)\pi^+(k_2)\,. \tag{A.1}$$

The z-axis is chosen in the Λ_b rest frame such that the Λ_c travels in positive and the W boson in negative z-direction. Within the Λ_c rest frame, we define the angle θ_{Λ_c} as the angle enclosed by the flight direction of the Λ baryon and the z-axis. Analogously, within the dilepton rest frame, θ_ℓ is defined as the angle between the charged lepton momentum and the z-axis. Finally, we define ϕ as the azimuthal angle of the π^+, i.e., if $\phi = 0$, the coordinate system is chosen such that the charged lepton and the π^+ both travel in positive x-direction.

JHEP12(2019)082

$\bar{\nu}(q_1)\ell^-(q_2)$-rest frame:

$$q_1^\mu = \begin{pmatrix} E_\nu \\ -|\mathbf{q}|\sin\theta_\ell \\ 0 \\ -|\mathbf{q}|\cos\theta_\ell \end{pmatrix}, \quad q_2^\mu = \begin{pmatrix} E_\ell \\ |\mathbf{q}|\sin\theta_\ell \\ 0 \\ |\mathbf{q}|\cos\theta_\ell \end{pmatrix}, \quad |\mathbf{q}| = \frac{q^2 - m_\ell^2}{2\sqrt{q^2}}\,. \tag{A.2}$$

The polarization vectors in this frame we choose to be

$$\epsilon^\mu(t) = (1,0,0,0)^T\,, \quad \epsilon^\mu(\pm) = \frac{1}{\sqrt{2}}(0,\pm 1,-i,0)^T\,, \quad \epsilon^\mu(0) = (0,0,0,-1)^T\,. \tag{A.3}$$

$\Lambda_c^+(k)$-rest frame:

$$k_1^\mu = \begin{pmatrix} E_\Lambda \\ -|\mathbf{k}|\sin\theta_{\Lambda_c}\cos\phi \\ -|\mathbf{k}|\sin\theta_{\Lambda_c}\sin\phi \\ |\mathbf{k}|\cos\theta_{\Lambda_c} \end{pmatrix}, \quad k_2^\mu = \begin{pmatrix} E_\pi \\ |\mathbf{k}|\sin\theta_{\Lambda_c}\cos\phi \\ |\mathbf{k}|\sin\theta_{\Lambda_c}\sin\phi \\ -|\mathbf{k}|\cos\theta_{\Lambda_c} \end{pmatrix}, \quad |\mathbf{k}| = \frac{\sqrt{\lambda(m_{\Lambda_c}^2, m_\Lambda^2, m_\pi^2)}}{2m_{\Lambda_c}}\,. \tag{A.4}$$

Furthermore, we define

$$\bar{q} = q_1 - q_2\,, \qquad \bar{k} = k_1 - k_2\,. \tag{A.5}$$

With these definitions, some of the kinematical Lorentz invariants are

$$\bar{q}\cdot\epsilon(\pm) = \pm\sqrt{\frac{q^2}{2}}\left(1 - \frac{m_\ell^2}{q^2}\right)\sin(\theta_\ell)\,, \tag{A.6}$$

$$\bar{q}\cdot\epsilon(0) = -\sqrt{q^2}\left(1 - \frac{m_\ell^2}{q^2}\right)\cos(\theta_\ell)\,, \tag{A.7}$$

$$\epsilon_{\mu\nu\lambda\rho}\epsilon^\mu(\pm)\epsilon^\nu(\mp)q_1^\lambda q_2^\rho = \pm\frac{i}{2}(q^2 - m_\ell^2)\cos(\theta_\ell)\,, \tag{A.8}$$

$$\bar{k}\cdot\epsilon(\pm) = \pm\sqrt{\frac{r_+ r_-}{2m_{\Lambda_c}^2}}\sin(\theta_{\Lambda_c})e^{\mp i\phi}\,, \tag{A.9}$$

$$\bar{k}\cdot\epsilon(0) = \frac{(m_\Lambda^2 - m_\pi^2)\sqrt{s_+ s_-} + (m_{\Lambda_b}^2 - m_{\Lambda_c}^2 - q^2)\sqrt{r_+ r_-}\cos(\theta_{\Lambda_c})}{2m_{\Lambda_c}^2\sqrt{q^2}}\,, \tag{A.10}$$

$$\epsilon_{\mu\nu\lambda\rho}\epsilon^\mu(\pm)\epsilon^\nu(\mp)k_1^\lambda k_2^\rho = \mp\frac{i}{2}\sqrt{r_+ r_-}\cos(\theta_{\Lambda_c})\,. \tag{A.11}$$

with $\epsilon^{0123} = -\epsilon_{0123} = +1$. We defined

$$r_\pm = (m_{\Lambda_c}^2 \pm m_\Lambda^2)^2 - m_\pi^2\,, \quad \text{such that} \quad r_+ r_- = \lambda(m_{\Lambda_c}^2, m_\Lambda^2, m_\pi^2)\,. \tag{A.12}$$

B Correlation matrices

We collect here the correlation matrices between the integrated angular observables K_i in the SM and in the selected benchmark points. The individual correlation coefficients have

JHEP12(2019)082

been obtained from the sample covariance using $2.5 \cdot 10^5$ samples. The sequence in which the observables appear is the same as in table 1.

The correlation matrix in the SM for $\ell = \mu$ reads

$$\begin{pmatrix} +1.000 & -0.680 & -0.110 & +0.130 & -0.191 & -0.175 & +0.266 \\ -0.680 & +1.000 & +0.047 & -0.213 & +0.125 & +0.350 & +0.020 \\ -0.110 & +0.047 & +1.000 & +0.962 & -0.953 & +0.899 & +0.862 \\ +0.130 & -0.213 & +0.962 & +1.000 & -0.982 & +0.797 & +0.876 \\ -0.191 & +0.125 & -0.953 & -0.982 & +1.000 & -0.847 & -0.945 \\ -0.175 & +0.350 & +0.899 & +0.797 & -0.847 & +1.000 & +0.825 \\ +0.266 & +0.020 & +0.862 & +0.876 & -0.945 & +0.825 & +1.000 \end{pmatrix} . \tag{B.1}$$

The correlation matrix in the SM for $\ell = \tau$ reads

$$\begin{pmatrix} +1.000 & -0.699 & -0.047 & -0.024 & -0.498 & -0.097 & +0.171 \\ -0.699 & +1.000 & +0.027 & -0.000 & +0.487 & +0.182 & -0.126 \\ -0.047 & +0.027 & +1.000 & +0.999 & -0.760 & +0.958 & +0.922 \\ -0.024 & -0.000 & +0.999 & +1.000 & -0.769 & +0.949 & +0.923 \\ -0.498 & +0.487 & -0.760 & -0.769 & +1.000 & -0.715 & -0.903 \\ -0.097 & +0.182 & +0.958 & +0.949 & -0.715 & +1.000 & +0.888 \\ +0.171 & -0.126 & +0.922 & +0.923 & -0.903 & +0.888 & +1.000 \end{pmatrix} . \tag{B.2}$$

The correlation matrix in the BMP #1 for $\ell = \tau$ reads

$$\begin{pmatrix} +1.000 & -0.703 & -0.047 & -0.025 & -0.673 & -0.100 & +0.162 \\ -0.703 & +1.000 & +0.027 & +0.004 & +0.649 & +0.165 & -0.109 \\ -0.047 & +0.027 & +1.000 & +1.000 & -0.532 & +0.958 & +0.934 \\ -0.025 & +0.004 & +1.000 & +1.000 & -0.543 & +0.951 & +0.935 \\ -0.673 & +0.649 & -0.532 & -0.543 & +1.000 & -0.495 & -0.741 \\ -0.100 & +0.165 & +0.958 & +0.951 & -0.495 & +1.000 & +0.896 \\ +0.162 & -0.109 & +0.934 & +0.935 & -0.741 & +0.896 & +1.000 \end{pmatrix} . \tag{B.3}$$

The correlation matrix in the BMP #2 for $\ell = \tau$ reads

$$\begin{pmatrix} +1.000 & -0.235 & -0.048 & -0.003 & -0.159 & -0.123 & +0.084 \\ -0.235 & +1.000 & -0.053 & -0.091 & +0.063 & +0.058 & +0.042 \\ -0.048 & -0.053 & +1.000 & +0.998 & -0.966 & +0.955 & +0.976 \\ -0.003 & -0.091 & +0.998 & +1.000 & -0.969 & +0.937 & +0.973 \\ -0.159 & +0.063 & -0.966 & -0.969 & +1.000 & -0.927 & -0.992 \\ -0.123 & +0.058 & +0.955 & +0.937 & -0.927 & +1.000 & +0.945 \\ +0.084 & +0.042 & +0.976 & +0.973 & -0.992 & +0.945 & +1.000 \end{pmatrix} . \tag{B.4}$$

JHEP12(2019)082

The correlation matrix in the BMP #3 for $\ell = \tau$ reads

$$\begin{pmatrix} +1.000 & -0.605 & +0.027 & -0.050 & -0.279 & -0.405 & +0.144 \\ -0.605 & +1.000 & -0.031 & -0.053 & +0.196 & +0.565 & -0.190 \\ +0.027 & -0.031 & +1.000 & +0.989 & -0.932 & +0.246 & +0.962 \\ -0.050 & -0.053 & +0.989 & +1.000 & -0.903 & +0.266 & +0.947 \\ -0.279 & +0.196 & -0.932 & -0.903 & +1.000 & -0.072 & -0.943 \\ -0.405 & +0.565 & +0.246 & +0.266 & -0.072 & +1.000 & +0.119 \\ +0.144 & -0.190 & +0.962 & +0.947 & -0.943 & +0.119 & +1.000 \end{pmatrix} . \tag{B.5}$$

References

[1] BaBar collaboration, *Evidence for an excess of $\bar{B} \to D^{(*)}\tau^-\bar{\nu}_\tau$ decays*, *Phys. Rev. Lett.* **109** (2012) 101802 [arXiv:1205.5442] [INSPIRE].

[2] BaBar collaboration, *Measurement of an excess of $\bar{B} \to D^{(*)}\tau^-\bar{\nu}_\tau$ decays and implications for charged Higgs bosons*, *Phys. Rev.* **D 88** (2013) 072012 [arXiv:1303.0571] [INSPIRE].

[3] Belle collaboration, *Measurement of the branching ratio of $\bar{B} \to D^{(*)}\tau^-\bar{\nu}_\tau$ relative to $\bar{B} \to D^{(*)}\ell^-\bar{\nu}_\ell$ decays with hadronic tagging at Belle*, *Phys. Rev.* **D 92** (2015) 072014 [arXiv:1507.03233] [INSPIRE].

[4] LHCb collaboration, *Measurement of the ratio of branching fractions $\mathcal{B}(\bar{B}^0 \to D^{*+}\tau^-\bar{\nu}_\tau)/\mathcal{B}(\bar{B}^0 \to D^{*+}\mu^-\bar{\nu}_\mu)$*, *Phys. Rev. Lett.* **115** (2015) 111803 [*Erratum ibid.* **115** (2015) 159901] [arXiv:1506.08614] [INSPIRE].

[5] Belle collaboration, *Measurement of the τ lepton polarization and $R(D^*)$ in the decay $\bar{B} \to D^*\tau^-\bar{\nu}_\tau$*, *Phys. Rev. Lett.* **118** (2017) 211801 [arXiv:1612.00529] [INSPIRE].

[6] Belle collaboration, *Measurement of the τ lepton polarization and $R(D^*)$ in the decay $\bar{B} \to D^*\tau^-\bar{\nu}_\tau$ with one-prong hadronic τ decays at Belle*, *Phys. Rev.* **D 97** (2018) 012004 [arXiv:1709.00129] [INSPIRE].

[7] LHCb collaboration, *Measurement of the ratio of the $B^0 \to D^{*-}\tau^+\nu_\tau$ and $B^0 \to D^{*-}\mu^+\nu_\mu$ branching fractions using three-prong τ-lepton decays*, *Phys. Rev. Lett.* **120** (2018) 171802 [arXiv:1708.08856] [INSPIRE].

[8] LHCb collaboration, *Test of lepton flavor universality by the measurement of the $B^0 \to D^{*-}\tau^+\nu_\tau$ branching fraction using three-prong τ decays*, *Phys. Rev.* **D 97** (2018) 072013 [arXiv:1711.02505] [INSPIRE].

[9] Belle collaboration, *Measurement of $\mathcal{R}(D)$ and $\mathcal{R}(D^*)$ with a semileptonic tagging method*, arXiv:1904.08794 [INSPIRE].

[10] M. Neubert, Z. Ligeti and Y. Nir, *The subleading Isgur-Wise form-factor $\chi_3(v, v')$ to order α_s in QCD sum rules*, *Phys. Rev.* **D 47** (1993) 5060 [hep-ph/9212266] [INSPIRE].

[11] Z. Ligeti, Y. Nir and M. Neubert, *The subleading Isgur-Wise form-factor $\chi_3(v, v')$ and its implications for the decays $\bar{B} \to D^*\ell\bar{\nu}$*, *Phys. Rev.* **D 49** (1994) 1302 [hep-ph/9305304] [INSPIRE].

JHEP12(2019)082

[12] S. Faller, A. Khodjamirian, C. Klein and T. Mannel, *$B \to D^{(*)}$ form factors from QCD light-cone sum rules*, *Eur. Phys. J.* **C 60** (2009) 603 [arXiv:0809.0222] [INSPIRE].

[13] S. Fajfer, J.F. Kamenik and I. Nisandzic, *On the $B \to D^* \tau \bar{\nu}_\tau$ sensitivity to new physics*, *Phys. Rev.* **D 85** (2012) 094025 [arXiv:1203.2654] [INSPIRE].

[14] HPQCD collaboration, *$B \to Dl\nu$ form factors at nonzero recoil and extraction of $|V_{cb}|$*, *Phys. Rev.* **D 92** (2015) 054510 [*Erratum ibid.* **D 93** (2016) 119906] [arXiv:1505.03925] [INSPIRE].

[15] MILC collaboration, *B to$D\ell\nu$ form factors at nonzero recoil and $|V_{cb}|$ from $2+1$-flavor lattice QCD*, *Phys. Rev.* **D 92** (2015) 034506 [arXiv:1503.07237] [INSPIRE].

[16] M. Neubert, Z. Ligeti and Y. Nir, *QCD sum rule analysis of the subleading Isgur-Wise form-factor Chi-2 (v v-prime)*, *Phys. Lett.* **B 301** (1993) 101 [hep-ph/9209271] [INSPIRE].

[17] D. Bigi and P. Gambino, *Revisiting $B \to D\ell\nu$*, *Phys. Rev.* **D 94** (2016) 094008 [arXiv:1606.08030] [INSPIRE].

[18] D. Bigi, P. Gambino and S. Schacht, *A fresh look at the determination of $|V_{cb}|$ from $B \to D^* \ell \nu$*, *Phys. Lett.* **B 769** (2017) 441 [arXiv:1703.06124] [INSPIRE].

[19] D. Bigi, P. Gambino and S. Schacht, *$R(D^*)$, $|V_{cb}|$ and the heavy quark symmetry relations between form factors*, *JHEP* **11** (2017) 061 [arXiv:1707.09509] [INSPIRE].

[20] Y.-M. Wang, Y.-B. Wei, Y.-L. Shen and C.-D. Lü, *Perturbative corrections to $B \to D$ form factors in QCD*, *JHEP* **06** (2017) 062 [arXiv:1701.06810] [INSPIRE].

[21] N. Gubernari, A. Kokulu and D. van Dyk, *$B \to P$ and $B \to V$ form factors from B-meson light-cone sum rules beyond leading twist*, *JHEP* **01** (2019) 150 [arXiv:1811.00983] [INSPIRE].

[22] P. Gambino, M. Jung and S. Schacht, *The V_{cb} puzzle: an update*, *Phys. Lett.* **B 795** (2019) 386 [arXiv:1905.08209] [INSPIRE].

[23] F.U. Bernlochner and Z. Ligeti, *Semileptonic $B_{(s)}$ decays to excited charmed mesons with e, μ, τ and searching for new physics with $R(D^{**})$*, *Phys. Rev.* **D 95** (2017) 014022 [arXiv:1606.09300] [INSPIRE].

[24] M. Bordone, G. Isidori and D. van Dyk, *Impact of leptonic τ decays on the distribution of $B \to P \mu \bar{\nu}$ decays*, *Eur. Phys. J.* **C 76** (2016) 360 [arXiv:1602.06143] [INSPIRE].

[25] F.U. Bernlochner, Z. Ligeti and D.J. Robinson, *Model independent analysis of semileptonic B decays to D^{**} for arbitrary new physics*, *Phys. Rev.* **D 97** (2018) 075011 [arXiv:1711.03110] [INSPIRE].

[26] P. Böer et al., *Testing lepton flavour universality in semileptonic $\Lambda_b \to \Lambda_c^*$ decays*, *JHEP* **06** (2018) 155 [arXiv:1801.08367] [INSPIRE].

[27] M. Blanke et al., *Impact of polarization observables and $B_c \to \tau\nu$ on new physics explanations of the $b \to c\tau\nu$ anomaly*, *Phys. Rev.* **D 99** (2019) 075006 [arXiv:1811.09603] [INSPIRE].

[28] LHCb collaboration, *Determination of the quark coupling strength $|V_{ub}|$ using baryonic decays*, *Nature Phys.* **11** (2015) 743 [arXiv:1504.01568] [INSPIRE].

[29] LHCb collaboration, *Measurement of the shape of the $\Lambda_b^0 \to \Lambda_c^+ \mu^- \overline{\nu}_\mu$ differential decay rate*, *Phys. Rev.* **D 96** (2017) 112005 [arXiv:1709.01920] [INSPIRE].

JHEP12(2019)082

[30] LHCb collaboration, *Measurement of b hadron fractions in 13 TeV pp collisions*, *Phys. Rev.* **D 100** (2019) 031102 [arXiv:1902.06794] [INSPIRE].

[31] A. Datta, S. Kamali, S. Meinel and A. Rashed, *Phenomenology of $\Lambda_b \to \Lambda_c \tau \overline{\nu}_\tau$ using lattice QCD calculations*, *JHEP* **08** (2017) 131 [arXiv:1702.02243] [INSPIRE].

[32] S. Shivashankara, W. Wu and A. Datta, *$\Lambda_b \to \Lambda_c \tau \bar{\nu}_\tau$ decay in the standard model and with new physics*, *Phys. Rev.* **D 91** (2015) 115003 [arXiv:1502.07230] [INSPIRE].

[33] T. Gutsche et al., *Semileptonic decay $\Lambda_b \to \Lambda_c + \tau^- + \bar{\nu_\tau}$ in the covariant confined quark model*, *Phys. Rev.* **D 91** (2015) 074001 [*Erratum ibid.* **D 91** (2015) 119907] [arXiv:1502.04864] [INSPIRE].

[34] P. Böer, T. Feldmann and D. van Dyk, *Angular analysis of the decay $\Lambda_b \to \Lambda(\to N\pi)\ell^+\ell^-$*, *JHEP* **01** (2015) 155 [arXiv:1410.2115] [INSPIRE].

[35] D. Das, *Model independent new physics analysis in $\Lambda_b \to \Lambda \mu^+ \mu^-$ decay*, *Eur. Phys. J.* **C 78** (2018) 230 [arXiv:1802.09404] [INSPIRE].

[36] D. Das, *On the angular distribution of $\Lambda_b \to \Lambda(\to N\pi)\tau^+\tau^-$ decay*, *JHEP* **07** (2018) 063 [arXiv:1804.08527] [INSPIRE].

[37] Particle Data Group collaboration, *Review of particle physics*, *Phys. Rev.* **D 98** (2018) 030001 [INSPIRE].

[38] S. Meinel, *$\Lambda_c \to \Lambda l^+ \nu_l$ form factors and decay rates from lattice QCD with physical quark masses*, *Phys. Rev. Lett.* **118** (2017) 082001 [arXiv:1611.09696] [INSPIRE].

[39] BESIII collaboration, *Measurements of Weak Decay Asymmetries of $\Lambda_c^+ \to pK_S^0$, $\Lambda\pi^+$, $\Sigma^+\pi^0$ and $\Sigma^0\pi^+$*, *Phys. Rev.* **D 100** (2019) 072004 [arXiv:1905.04707] [INSPIRE].

[40] S. Descotes-Genon et al., *The CKM parameters in the SMEFT*, *JHEP* **05** (2019) 172 [arXiv:1812.08163] [INSPIRE].

[41] CLEO collaboration, *Measurement of the Λ_c decay asymmetry parameter*, *Phys. Rev. Lett.* **65** (1990) 2842 [INSPIRE].

[42] ARGUS collaboration, *A measurement of asymmetry in the decay $\Lambda_c^+ \to \Lambda\pi^+$*, *Phys. Lett.* **B 274** (1992) 239 [INSPIRE].

[43] CLEO collaboration, *Measurement of the decay asymmetry parameters in $\Lambda_c^+ \to \Lambda\pi^+$ and $\Lambda_c^+ \to \Sigma^+\pi^0$*, *Phys. Lett.* **B 350** (1995) 256 [hep-ex/9502004] [INSPIRE].

[44] FOCUS collaboration, *Study of the decay asymmetry parameter and CP-violation parameter in the $\Lambda_c^+ \to \Lambda\pi^+$ decay*, *Phys. Lett.* **B 634** (2006) 165 [hep-ex/0509042] [INSPIRE].

[45] T. Feldmann and M.W.Y. Yip, *Form factors for $\Lambda_b \to \Lambda$ transitions in SCET*, *Phys. Rev.* **D 85** (2012) 014035 [*Erratum ibid.* **D 86** (2012) 079901] [arXiv:1111.1844] [INSPIRE].

[46] G. Ciezarek, A. Lupato, M. Rotondo and M. Vesterinen, *Reconstruction of semileptonically decaying beauty hadrons produced in high energy pp collisions*, *JHEP* **02** (2017) 021 [arXiv:1611.08522] [INSPIRE].

[47] LHCb collaboration, *Physics case for an LHCb upgrade II — Opportunities in flavour physics and beyond, in the HL-LHC era*, arXiv:1808.08865 [INSPIRE].

[48] D. van Dyk et al., *EOS — A HEP program for flavor observables*, version 0.3, available from https://eos.github.io.

JHEP12(2019)082

[49] C. Murgui, A. Peñuelas, M. Jung and A. Pich, *Global fit to $b \to c\tau\nu$ transitions*, *JHEP* **09** (2019) 103 [arXiv:1904.09311] [INSPIRE].

[50] W. Detmold, C. Lehner and S. Meinel, *$\Lambda_b \to p\ell^-\bar{\nu}_\ell$ and $\Lambda_b \to \Lambda_c\ell^-\bar{\nu}_\ell$ form factors from lattice QCD with relativistic heavy quarks*, *Phys. Rev.* **D 92** (2015) 034503 [arXiv:1503.01421] [INSPIRE].

[51] F.U. Bernlochner, Z. Ligeti, D.J. Robinson and W.L. Sutcliffe, *Precise predictions for $\Lambda_b \to \Lambda_c$ semileptonic decays*, *Phys. Rev.* **D 99** (2019) 055008 [arXiv:1812.07593] [INSPIRE].

JHEP12(2019)082